




Ionic current blockade in a nanopore due to an ellipsoidal particle

Dmitriy V. Melnikov , Nelson R. Barker , and Maria E. Gracheva ^{*}
Department of Physics, Clarkson University, Potsdam, New York 13699, USA

 (Received 13 May 2024; accepted 9 August 2024; published 3 September 2024)

Nanopores in solid-state membranes have been used to detect, identify, filter, and characterize nanoparticles and biological molecules. In this work, we simulate an ionic flow through a nanopore while an ellipsoidal nanoparticle translocates through a pore. We numerically solve the Poisson-Nernst-Planck equations to obtain the ionic current values for different aspect ratios, sizes, and orientations of a translocating particle. By extending the existing theoretical model for the ionic current in the nanopore to the particles of ellipsoidal shape, we propose semiempirical fitting formulas which describe our computed data within 5% accuracy. We also demonstrate how the derived formulas can be used to identify the dimensions of nanoparticles from the available experimental data which may have useful applications in bionanotechnology.

DOI: [10.1103/PhysRevE.110.034403](https://doi.org/10.1103/PhysRevE.110.034403)

I. INTRODUCTION

Since 1950s [1–3], porous membranes have been used to characterize microscopic and nanoscopic objects of various shapes and dimensions, e.g., nanoparticles and nanorods made of various materials, filamental viruses, and biomolecules, such as DNA [4–9]. Nanopores in solid-state membranes are of particular interest as their dimensions can be customized for a problem at hand [10]. To perform a measurement, a membrane with a nanopore in it is used to separate two reservoirs filled with an electrolyte solution so that when an electric bias is applied across the membrane, the ionic current flows the pore. The same bias can also facilitate a passage of a charged particle through the nanopore while for an uncharged or weakly charged objects, the translocation can be achieved by a variety of other means such as, for example, by creating a pressure driven flow or utilizing the electroosmotic flow of the fluid through nanopore carrying a surface charge [11]. Regardless of a particular transport mechanism, a nanoparticle traversing through a nanopore affects the ionic current, and the change in current which, in general, depends on the particle’s size, shape [12], location [13], and orientation inside the nanopore [14–16] can be then recorded using a resistive pulse technique [2,17–20].

To gain insight into how the ionic current depends on the translocating nanoparticles properties, we first consider a simple model where the nanopore system is represented as a series of three Ohmic resistors connected in series [2], which are the two access resistances [21] near the nanopore ends, and the resistance of the nanopore itself. The access resistances appear due to bending of the current streamlines in the inlet and outlet regions of the nanopore. The resistance of a cylindrical pore depends on its length, L , and the diameter, D . When the particle is present in the pore, the volume of the pore open to the current flow decreases resulting in the reduction of

the ionic current I_b from its open pore value, I_o , observed when the nanoparticle is not present. In the limit of a small nanoparticle in a long nanopore with $L \gg D$ so that the nanoparticle can fit completely within the pore without affecting the current flow around the nanopore [22], the relative change in the ionic current, or the “ionic current blockade” $(I_o - I_b)/I_o = \Delta I/I_o$, is proportional to the ratio of the volumes of the nanoparticle and nanopore, v and V , respectively [2,20]:

$$\frac{\Delta I}{I_o} = f \frac{v}{V} \frac{1}{1 + \pi D/(4L)} \equiv f\Omega, \quad (1)$$

where parameter Ω lumps together the volume ratio v/V and the finite nanopore length factor $[1 + \pi D/(4L)]^{-1}$. Factor f in this equation is the electric shape factor [2,14,23,24] which depends on the nanoparticles’ shape, orientation, and position inside the pore. For spherical particles, $f = 3/2$ [2]. For ellipsoidal particles the shape factor is strongly dependent on the particle’s dimensions [14,23,24], and for an arbitrary angle θ between the axes of revolution of a spheroidal particle and the nanopore, it can be written as [14]

$$f = f_{\parallel} + (f_{\perp} - f_{\parallel}) \sin^2(\theta), \quad (2)$$

where f_{\parallel} (f_{\perp}) is the shape factor of the particle with the axis of revolution parallel (perpendicular) to the pore axis [14,23,24].

The above discussion and the resulting Eq. (1), are approximate, that is, strictly speaking, they are only valid in the limit of small nanoparticles with $v \ll V$ which are also assumed to be moving through the nanopore along its central axis. In this case, the uniform electric field lines (or the current streamlines) in the nanopore due to the applied bias bend around the small nanoparticle while remaining largely unaffected along the nanopore walls. Increasing the dimensions of a translocating object and/or moving it off-axis strongly modifies the electric field in the nanopore particularly in the annular region between the particle and the nanopore as the current streamlines have to be confined to the nanopore. This results in the decrease of the ionic current below the values

^{*}Contact author: gracheva@clarkson.edu

predicted by the small-particle limit of Eq. (1) [13,25–27]. The above equation also omits the effects on the ionic current from the electric charge frequently accumulated on surfaces of the nanoparticle and/or nanopore. The charge distribution on the nanoparticle and nanopore surfaces strongly affects the ionic current leading, for example, to the increase of the ionic current above the open pore baseline under certain conditions; these effects were discussed elsewhere [28,29].

In this work, our main aim is to analyze the ionic current blockade arising due to “large” dielectric particles of ellipsoidal shape with dimensions larger or comparable to the nanopore diameter. We focus on the ellipsoidal particles because many biological macromolecules can be approximated with that shape [13] which may facilitate the analysis of the experimental data. On the other hand, nanoparticles in the shape of rods or cylinders (nanorods) as well as some filamental viruses [5,7,30] can also be modelled as very slender ellipsoids.

To this end, we first perform calculations based on the current conservation inside the nanopore in order to establish the leading term dependence of the large-particle-size correction factor to the ionic current predicted by Eq. (1). The calculations are similar to the method originally proposed in Ref. [2] for spherical particles which considers contribution to the ionic current only from the current streamlines confined completely within the nanopore volume. We then use these results to construct the fitting formulas for the ionic current blockade ratios $\Delta I/I_o$ obtained from numerical calculations utilizing the self-consistent solution of the Poisson-Nernst-Planck (PNP) system of equations [29,31] for a broad range of particle and pore dimensions. We perform calculations of the ionic current blockade for the particle positioned along the central axis or off-center and for different orientations of the nanoparticle within the nanopore, and provide corresponding large-particle correction factors for these cases, thus providing a comprehensive description of the ionic current response to the translocation of the ellipsoidal particle through the nanopore.

The paper is organized as follows. Section II describes the semiempirical model of the ionic current response to large particles while Sec. III describes our simulated nanopore-nanoparticle system and the PNP model we use to numerically calculate the ionic current. Section IV presents and discusses the simulation results and their analysis with the help of formulas derived using the model of Sec. II. The final Sec. V summarizes the results and briefly outlines the future work. Details of the semiempirical calculations of the ionic current blockade for large ellipsoidal particles and the model validation are relegated to Appendixes A and B, respectively.

II. IONIC CURRENT BLOCKADE FOR LARGE TRANSLOCATING PARTICLES

For a small, neutral, dielectric particle translocating through a long cylindrical nanopore, neglecting the access resistance contribution, the blocked pore ionic current I_b is equal to [24,29]

$$I_b^{(1)} = I_o \left(1 - 4 \frac{\oint_{a_p} \phi_0 \hat{z} \cdot d\vec{a}}{\pi D^2 \Delta V} \right), \quad (3)$$

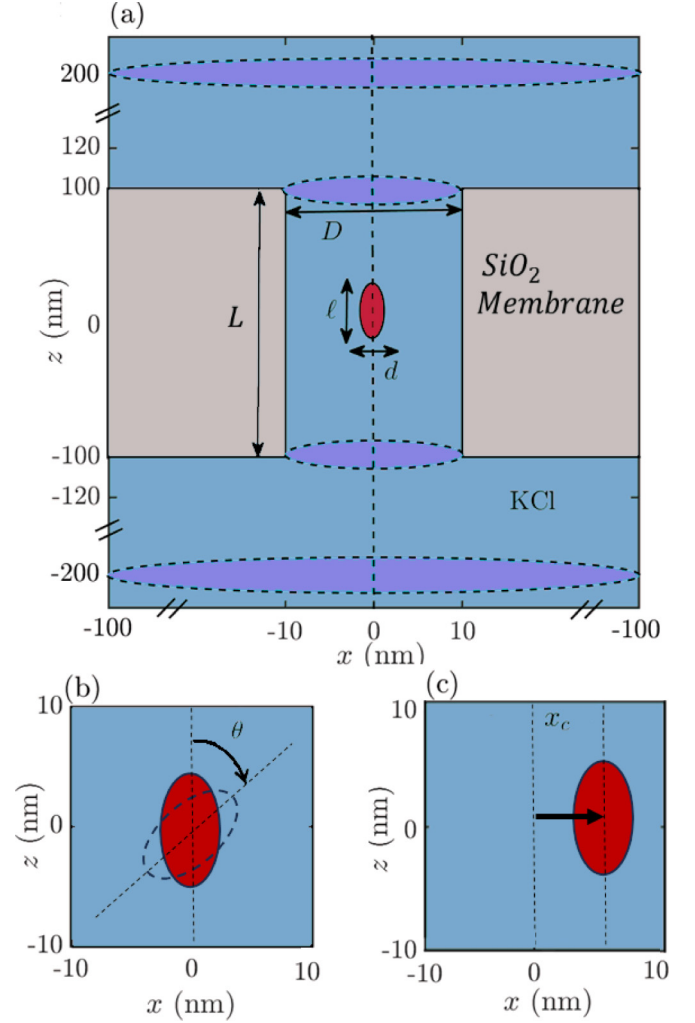


FIG. 1. Schematic representation of (a) the membrane-nanopore system shown in a cross section (see Sec. III A for detailed explanation of symbols), (b) the nanoparticle oriented at an angle θ relative to the pore’s z axis, and (c) the nanoparticle in an off-axis position at a distance x_c from the pore’s z axis.

where the integration of the electric potential ϕ_0 is performed over the surface of the nanoparticle a_p , and in derivation of this equation it is assumed that the nanoparticle does not perturb the electric potential difference ΔV applied across the nanopore.

In principle, the electric potential ϕ_0 in the above equation should be evaluated numerically from the solution of the PNP equations. However, for a small uncharged spherical nanoparticle in the uniform electric field far away from the nanopore walls, the approximate closed form solution for ϕ_0 can be written as

$$\phi_0 = -E \cos \theta \left(r + \frac{d^3}{16r^2} \right), \quad (4)$$

where r is the distance from the particle’s center and angle θ is measured from the z axis of the pore (see Fig. 1 where the membrane-nanopore system is schematically represented). Substituting this expression in Eq. (3) and evaluating the

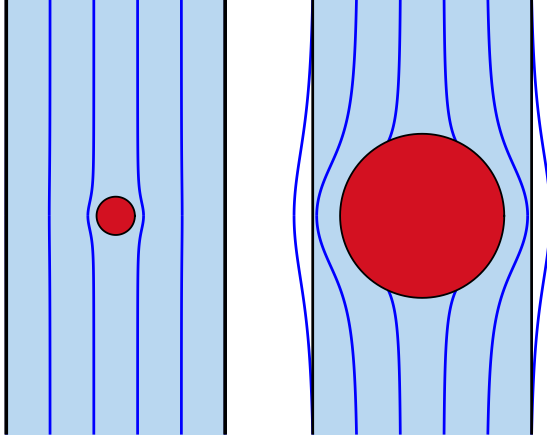


FIG. 2. Current streamlines (dark blue) calculated from Eq. (4) in a nanopore with a spherical particle (red) for two different particle's sizes. The "leakage" of the streamlines outside the nanopore is visible for the large particle.

surface integral then gives [2,24]

$$I_b^{(1)} = I_o \left(1 - \frac{Ed^3}{\Delta VD^2} \right). \quad (5)$$

If we further set E equal to the value of the uniform electric field in the nanopore, $E = \Delta V/L$, then we recover Eq. (1) with the shape factor $f = 3/2$.

On the other hand, in general, the ionic current through any cross-sectional area of the pore, A_p , can also be evaluated from the Ohm's law as

$$I_b = \sigma \int_{A_p} E_z da, \quad (6)$$

where σ is the electrolyte's solution conductivity (constant in our case), and $E_z = -\nabla\phi_0 \cdot \hat{z}$ is the component of the electric field along the nanopore z axis. In presence of the spherical nanoparticle, at the position of the maximum nanopore constriction, $z = 0$, with the electric potential given by Eq. (4), we then find that

$$I_b^{(2)} = \frac{\pi\sigma ED^2}{4} \left[1 - \left(\frac{d}{D} \right)^3 \right] = \frac{I_o EL}{\Delta V} \left[1 - \left(\frac{d}{D} \right)^3 \right], \quad (7)$$

where the open pore current for a cylindrical nanopore is $I_o = \sigma \Delta V \pi D^2 / (4L)$.

Clearly, $I_b^{(1)}$ and $I_b^{(2)}$ should be equal. For small nanoparticles, $d \ll D$, the difference between $I_b^{(1)}$ and $I_b^{(2)}$ is slight, but with increasing particle's size, $I_b^{(1)}$ and $I_b^{(2)}$ begin to deviate with $I_b^{(2)} < I_b^{(1)}$ in long pores with $L > D$. This is because, for larger nanoparticles, Eq. (4) is not an acceptable solution for the electric potential as the current streamlines due to it cannot be confined inside the nanopore in the annular region around the nanoparticle (see Fig. 2).

We can resolve this difficulty by requiring $I_b^{(1)} = I_b^{(2)}$ and treating E as an adjustable parameter. For the long pores ($D \ll L$), the second term in Eq. (5) can be neglected, thus leading to $E \approx (\Delta V/L) / [1 - (d/D)^3]$. Substituting this E back into

Eq. (5) gives

$$I_b \approx I_o \left(1 - f \frac{v}{V} \left[1 - \left(\frac{d}{D} \right)^3 \right]^{-1} \right), \quad (8)$$

and the ionic current blockade ratio

$$\frac{\Delta I}{I_o} = f \frac{v}{V} F \left[\left(\frac{d}{D} \right)^3 \right], \quad (9)$$

which is larger than the small-particle result of Eq. (1) by a factor $F[(d/D)^3] = [1 - (d/D)^3]^{-1}$.

We should emphasize that the above approach only establishes that the large-particle-size correction term F for spherical nanoparticles is $\sim (d/D)^3$, $F[(d/D)^3]$, and does not provide a correct numerical form of the dependence. That task is accomplished by fitting the numerical calculations described in the next section to this dependence. The above is also equivalent to calculations in Ref. [2] based on conservation of the number of the ionic current density streamlines (to keep constant current value) through a nanopore with a nanoparticle.

Performing similar calculations for spheroidal particles, we find that (see Appendix A for details) for a large oblate spheroid translocating through the nanopore, the large-particle correction factor strongly depends on its orientation in the nanopore changing from $F[(d/D)^3]$ when its axis revolution is along the nanopore axis to $F[l d^2/D^3]$ when they are perpendicular. For the prolate spheroid, the correction factor dependence varies from $F[(d/D)^2]$ for long particles to $F[l d^2/D^3]$ for small and slender ones.

III. COMPUTATIONAL MODEL AND METHOD

A. Nanopore model

In this work we consider a thin nanometer-scale silicon dioxide (SiO_2) membrane carrying a cylindrical nanopore which connects reservoirs, above and below the membrane, filled with an electrolyte solution (Fig. 1). The reservoirs are large compared to the membrane thickness, and filled with a potassium chloride (KCl) solution.

The membrane thickness (the pore length) is denoted by L and nanopore diameter is D . An ellipsoidal nanoparticle, placed in the nanopore center with its center at $z = 0$, is shown in Fig. 1 as well. The nanoparticle has length ℓ and diameter d . The angular orientation of the nanoparticle in the pore is varied from $\theta = 0^\circ$ to 90° , where $\theta = 0^\circ$ is when the particle's axis of revolution is parallel to the nanopore axis (z axis), and 90° is when the particle's vertical axis is normal to the z axis, see Fig. 1(b). The particle's off-axis position is also varied; Fig. 1(c) shows the nanoparticle at some off-axis distance x_c from the nanopore axis.

Ions within the electrolyte solution move across the membrane via the nanopore in the presence of the applied electric potential bias producing an ionic current. The electric potential ϕ and the ionic flux density \vec{N}_i are described by the PNP model:

$$\nabla^2 \phi = -\frac{eN_A}{\epsilon_o \epsilon_r} (z_+ c_+ + z_- c_-), \quad (10)$$

$$\nabla \cdot \vec{N}_i = 0, \quad (11)$$

$$\vec{N}_i = D_i \left(\nabla c_i + \frac{e z_i}{k_b T} c_i \nabla \phi \right). \quad (12)$$

Here subscript $i = +, -$ denotes the positive (K^+) and negative (Cl^-) ion species in the electrolyte, c_i is the local concentration of the corresponding ions, e is the elementary charge, k_b is Boltzmann constant, $T = 293.15$ K is temperature, N_A is Avogadro number, $\epsilon_r = 78$ is the solution's relative permeability, ϵ_o is the permittivity of free space, z_i is valency of the electrolyte ions ($z_i = \pm 1$ here), D_i are the ions' diffusion coefficients, $D_{Cl^-} = 2.03 \times 10^{-9}$ m²/s and $D_{K^+} = 1.95 \times 10^{-9}$ m²/s.

An electrolyte bias ΔV is set across the membrane by maintaining a 100 mV potential at the bottom reservoir boundary and 0 mV at the top reservoir boundary. For the Poisson Eq. (10), on the side reservoir surfaces, we set the normal component of the electric field to zero,

$$\hat{n} \cdot \nabla \phi = 0, \quad (13)$$

where \hat{n} is a unit vector normal to the boundary surface. Since the dielectric constant of both the nanoparticle and membrane is much smaller than that of the solution (3.9 vs 78), this leads to their small induced polarization which allows to use Eq. (13) on the membrane-electrolyte (zero charge on the membrane) and on the nanoparticle-electrolyte (no charge on the particle) interfaces as well [32].

For the Nernst-Planck Eq. (11), the normal component of the ionic flux is set to zero on the membrane-electrolyte, the nanoparticle-electrolyte interfaces, and the side boundaries of the reservoirs, while on the top and bottom of the reservoirs (inlet and outlet) the constant bulk ionic concentration $c_b = 0.1$ M is maintained.

The ionic current flowing through the nanopore is calculated from the ionic flux densities \vec{N}_i , see Eq. (12), for the two species as follows:

$$I = e N_A \int_S (z_+ \vec{N}_+ + z_- \vec{N}_-) \cdot d\vec{S}, \quad (14)$$

where the integral is evaluated over the surface area S at the upper boundary of the top reservoir. Because the ionic blockade ratio remains constant when the uncharged particle is fully inside the uncharged nanopore [29] away from its ends, in what follows, we always place the nanoparticle at $z = 0$ (Fig. 1) when calculating the blocked pore ionic current I_b .

B. Two-dimensional simulations

When the nanoparticle is located in the center of the pore with nanoparticle's axis of revolution lined up with the pore's z axis ($\theta = 0^\circ$), due to cylindrical symmetry of our nanopore-membrane system described in Sec. III A, the PNP Eqs. (10) and (11) can be solved numerically in two dimensions (2D) on the computational domain shown in Fig. 3. Here the membrane thickness (the pore length) is $L = 200$ nm and nanopore diameter is $D = 20$ nm, the electrolyte reservoirs are 100 nm in height and 200 nm in width each. Throughout this work, we use Comsol Multiphysics 5.3 to obtain the numerical solution of our PNP model. The mesh utilized in the 2D model is a

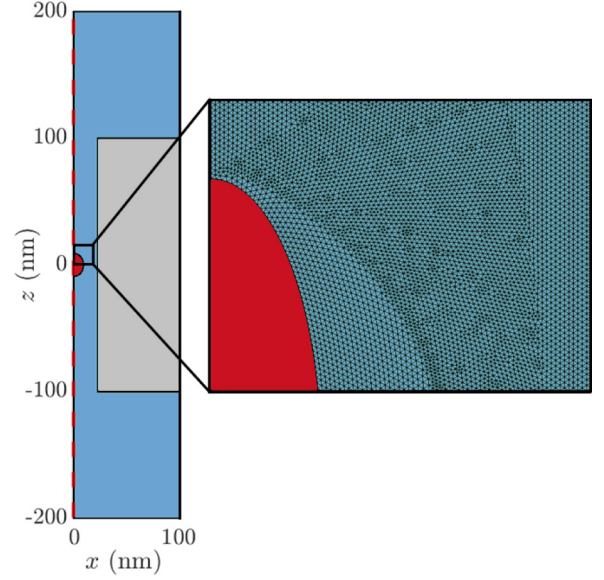


FIG. 3. Two-dimensional simulation domain. The inset shows a magnified portion of the nanoparticle-nanopore with superimposed mesh.

free triangular mesh with a fixed size of 0.1 nm which results in approximately 2×10^7 mesh elements.

C. Three-dimensional simulations

To calculate the ionic current for nonzero values of the angle θ between the nanoparticle's axis of revolution and the nanopore z axis [Fig. 1(b)] or when the particle is located off-center in the nanopore [Fig. 1(c)], a 3D computational model of the system is built (Fig. 4). With the addition of an extra dimension, the number of mesh elements increases dramatically. Because of this, all dimensions of the system have to be scaled down by an order of magnitude to make the solution feasible by the Comsol solver, so that the nanopore

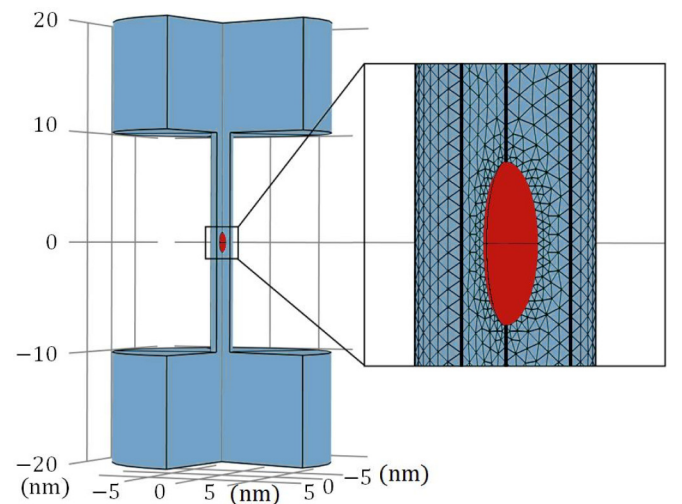


FIG. 4. Three-dimensional simulation domain with a slice removed to visualize the interior. The inset shows a magnified portion of the nanoparticle-nanopore with mesh.

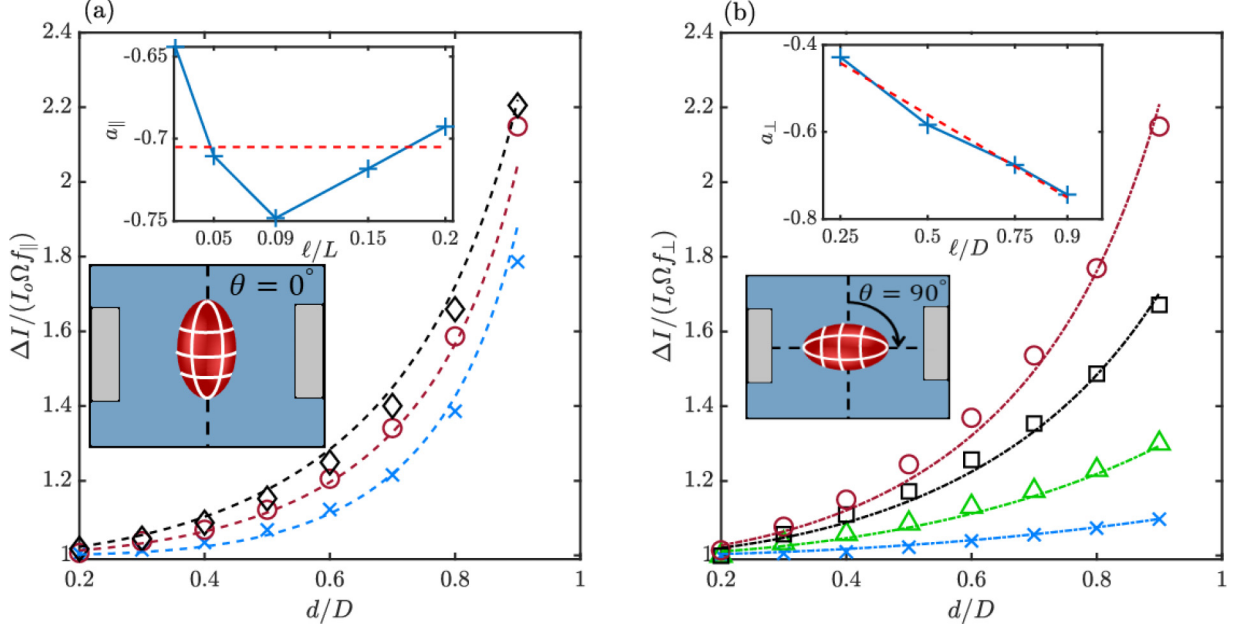


FIG. 5. (a) Normalized ionic current blockade ratio $\Delta I / (I_o \Omega f_{\parallel})$ for spheroids with the axis of revolution oriented parallel to the nanopore axis for different particle lengths ℓ . Symbols represent the results of calculations while the dashed curves are the results of the fitting with Eq. (15): Blue \times symbols and curve corresponds to $\ell/L = 0.025$, red \circ and curve – $\ell/L = 0.09$, and black \diamond and curve – $\ell/L = 0.2$. The inset shows dependence of the parameter a_{\parallel} on the length ℓ with a horizontal dashed line drawn at the best fit value. (b) Same as in (a) but for the perpendicular orientation of the nanoparticle ($\theta = 90^\circ$) with Eq. (16) used to generate the fitting curves. Blue \times symbols and curve corresponds to $\ell/L = 0.025$, black \triangleright and curve – $\ell/L = 0.05$, and red \circ and curve – $\ell/L = 0.09$. The inset shows $a_{\perp}(\ell)$ dependence with the best fit (dashed) line.

now has a length of $L = 20$ nm and a diameter $D = 2$ nm. The dimensions of the spheroidal particle are also varied accordingly. As the current blockade expression is expected to depend only on the ratios of the nanoparticle-nanopore dimensions, this scaling does not affect the value of $\Delta I / I_o$; this was verified by comparing results of 2D calculations against 3D data for the appropriate cases with a nanoparticle in the on-axis position and $\theta = 0$ (see Appendix B). The mesh utilized for this model is a custom free triangular mesh with a minimum mesh size of 0.05 nm in the nanopore that grows gradually to a maximum mesh size 0.4 nm in reservoirs and creates approximately 3×10^6 mesh elements in total. The relative tolerance for the Comsol solver is set to 10^{-6} in both 2D and 3D simulations.

IV. RESULTS AND DISCUSSION

A. Ionic current blockade

1. On-axis position of the nanoparticle

In Fig. 5 the normalized ionic current blockade, $\Delta I / (I_o \Omega f_{\parallel(\perp)})$, which is equal to the the large-particle factor, see Eq. (9), is shown for ellipsoidal particles of various lengths and diameters when the particle's axis of revolution is Fig. 5(a) parallel and Fig. 5(b) perpendicular to the nanopore axis. According to the discussion in Sec. I, the ratio $\Delta I / (I_o \Omega f_{\parallel(\perp)})$ gives the large-particle factor (correction) to the ionic current blockade which, as can be seen in this figure, approaches unity for small particles and increases with the particle diameter and length. For example, in Fig. 5(a), when the particle's diameter is about half of the pore's diameter

($d/D \sim 0.5$), this correction is $\sim 10\%$, and it rapidly grows to $\sim 200\%$ for $d/D = 0.9$. One can also immediately see that for the parallel orientation of particles, the dependence of $\Delta I / (I_o \Omega f_{\parallel})$ on the nanoparticle length ℓ is rather weak: All curves for different ratios ℓ/L are close together, and the ionic current blockade ratio changes only by $\sim 20\%$ when the particle's length varies from $\ell/L = 0.025$ to 0.2 for the particles with $d/D = 0.9$. Qualitatively this could be understood by noting that for a fixed d/D the cross-sectional area of the nanopore open to the current flow is the same irrespective of the particle's length ℓ . At the same time, the electric field at the position of the ellipsoid's center ($z = 0$) becomes more aligned along the nanopore's axis due to the decrease in the particle's surface curvature with increasing ℓ as the spheroid starts to look like a long cylinder. Quantitatively, this behavior is described by Eq. (A3) of the Appendix. Note also that we limited our particle length to $\ell/L = 0.2$ as increasing it further begins to perturb the access resistances of the nanopore so that factor Ω becomes dependent on the nanoparticle dimensions [22].

We should also note that individual curves for different ℓ values in Fig. 5 do not correspond to either prolate or oblate shapes of the particles, rather, for most of them, when the particle's diameter increases, the particle's shape transitions from oblate to prolate. In other words, the limiting cases considered in Appendix A separately for different shapes can only serve as a guidance when constructing a fitting formulas for the ionic current blockade curves valid in the broad range of the nanoparticle dimensions. Keeping in mind that the equations for the large-particle factor F in Appendix A all have the same common factor $(d/D)^2$, we propose the following fitting

formula for the large-particle corrections in the case of the parallel orientation of the spheroid along the nanopore axis:

$$\frac{\Delta I}{I_o \Omega f_{\parallel}} = \left[1 - a_{\parallel} \frac{d^n + \ell^n}{D^n + \ell^n} \left(\frac{d}{D} \right)^2 \right]^{-1}, \quad (15)$$

where we found that for $n = 2$, the fitting parameter a_{\parallel} is practically independent of the particle's length ℓ , see inset to Fig. 5(a). Setting $a_{\parallel} = 0.71$ (dashed line in the inset) provides the best fit to all computed data (within 4%), with corresponding fits shown in Fig. 5(a) as dashed curves.

When the spheroid is oriented perpendicular to the nanopore axis, the large-particle corrective term exhibits a much stronger dependence on its length ℓ as seen in Fig. 5(b). Here shorter particles with smaller values of ℓ exhibit smaller corrections than longer ones for the same value of the particle's diameter. This can be easily understood by noting that in this orientation of the particle, increasing ℓ for a fixed d decreases the area of the nanopore cross section open to the ionic current resulting in a smaller number of the current streamlines that can fit in it.

In constructing a fitting formula for the data in Fig. 5(b), we expect, based on the limiting cases discussed in Appendix A for the perpendicular orientation of the nanoparticle, that the resulting equation for $\Delta I / (I_o \Omega f_{\perp}) \sim [1 - a_{\perp} (\ell d^2 / D^3)]^{-1}$. The computed values of a_{\perp} are shown in the inset in Fig. 5(b). One can see that they can be well fitted with a linear function of ℓ / D so that the proposed fitting formula has the form:

$$\frac{\Delta I}{I_o \Omega f_{\perp}} = \left[1 - \left(a_{1\perp} + a_{2\perp} \frac{\ell}{D} \right) \frac{\ell d^2}{D^3} \right]^{-1}, \quad (16)$$

where the best fit values for $a_{1\perp} = 0.32$ and $a_{2\perp} = 0.48$. The large-particle corrections calculated with this formula are shown in Fig. 5(b) as dashed curves; they agree with the computed data within 4%.

We now consider how the large particles affect the ionic current blockade for the arbitrary orientation in the pore assuming that they are on the nanopore axis. In Fig. 6, the dependence of the ionic blockade ratio $\Delta I / I_o$ vs the orientation angle θ , $0 < \theta < 90^\circ$, between the particle's axis of revolution and the nanopore axis is shown for the same length values ℓ as in the last figure and for a few particle diameters. Here the data for $\theta = 0$ and 90° correspond to those shown in Fig. 5 multiplied by the shape factors f_{\parallel} and f_{\perp} , respectively. Overall, this plot conforms to the conclusions made above, specifically, that the largest orientation induced changes in the ionic current occur for the flat oblate spheroids [smallest value of ℓ / L , Fig. 6(a)] and the closer the particle's shape to the spherical, the less is $\Delta I / I_o$ dependence on its orientation.

The data shown in this plot, in analogy to the small-particle limit, Eq. (2), can be fitted as

$$\frac{\Delta I}{I_o \Omega} = f_{\parallel}^* + (f_{\perp}^* - f_{\parallel}^*) \sin^2(\theta) \quad (17)$$

with $f_{\parallel(\perp)}^*$ defined through the shape factors $f_{\parallel(\perp)}$ [14] and the normalized ionic current blockade values at $\theta = 0$ and 90° given by Eqs. (15) and (16) as

$$f_{\parallel(\perp)}^* = f_{\parallel(\perp)} \left(\frac{\Delta I}{I_o \Omega f_{\parallel(\perp)}} \right). \quad (18)$$

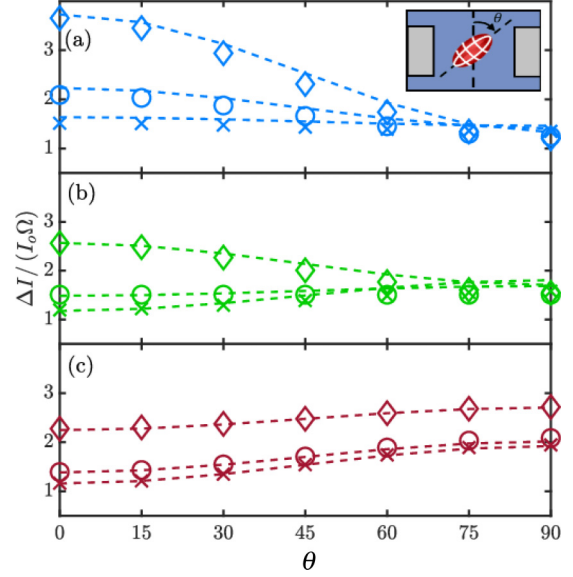


FIG. 6. The ionic current blockade ratio $\Delta I / I_o$ vs orientation angle θ . Symbols are the results of the calculations, the dashed curves are from Eq. (17) with the corrections proposed by Eqs. (15) and (16) for the particle length (a) $\ell / L = 0.025$, (b) $\ell / L = 0.05$, and (c) $\ell / L = 0.09$. In each plot, \times correspond to $d / D = 0.3$, \circ - $d / D = 0.5$, and \diamond - $d / D = 0.8$.

The results of this fitting formula are shown as dashed curves in Fig. 6 and are in excellent agreement with numerically computed values. This means that using our proposed fitting formulas for the perpendicular and parallel orientations of the nanoparticle's axis of revolution relative to the nanopore axis, we can accurately predict the ionic current blockade values for large ellipsoidal particles at arbitrary angular orientation in the nanopore.

2. Off-axis position of the nanoparticle

When a nanoparticle permeates through a nanopore, in general, it can also be found at different radial positions within the nanopore [see Fig. 1(c)]. The particle's position affects the electric field and potential distribution in the nanopore, and consequently, the ionic current. As shown in Fig. 7, as particle gets closer to a nanopore wall, the electric field component along the nanopore's axis, E_z , between the spheroid and the nanopore's wall nearest to it increases above the values found when the particle is on the central axis. On the opposite side of the particle, away from it, the electric field decreases below the values for the symmetric placement of the nanoparticle [cf. panels (c) and (a) in Figs. 7(c) and 7(a)]. When integrated over the whole cross-sectional area of the nanopore, see Eq. (6), this redistribution of the electric field results in the overall decrease of the blocked pore ionic current relative to the values for the on-axis position of the particle (the ionic current blockade ratio increases), and the further the particle's off-center displacement, the stronger the blockade.

This behavior is illustrated in Fig. 8 where it is shown how the ionic current changes when the nanoparticles of various dimensions are moved off-axis. Here we plot the ratio of the ionic current change when the particle's center is displaced

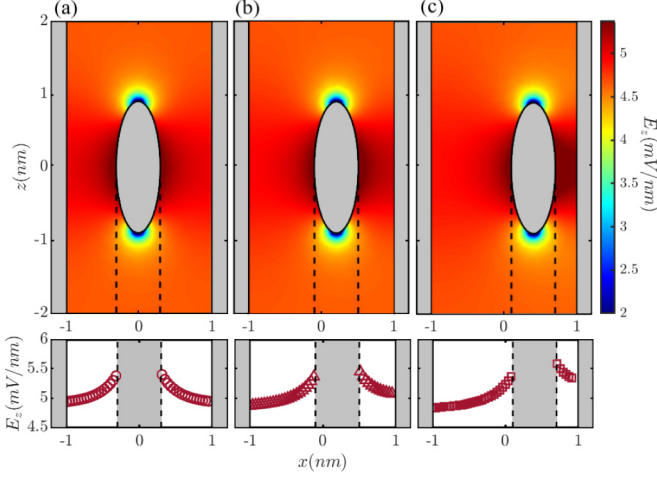


FIG. 7. Top row: Two-dimensional distribution z component of the electric field, E_z , in the vicinity of the translocating spheroid of length $\ell/L = 0.09$ and diameter $d/D = 0.3$ for three different radial positions of the particle in the nanopore: (a) $x_c = 0$, (b) $x_c = 0.1D$, and (c) $x_c = 0.2D$. Bottom row: E_z along the x direction for $z = 0$. Vertical dashed lines show nanoparticle's edges in the x direction.

from the cylindrical nanopore's axis by distance x_c along the x direction, $\Delta I(x_c) = I_o - I(x_c)$, to the current change $\Delta I(0) = I_o - I(0)$ when the nanoparticle is on the pore's axis. One can see from the plot that the longer the spheroid, the smaller the change in the current. In fact, for all presented cases, the increase in the ionic current is quite small, less than 5%, when the particle's point closest to the nanopore surface is at 10% of the pore's diameter from it. This indicates that

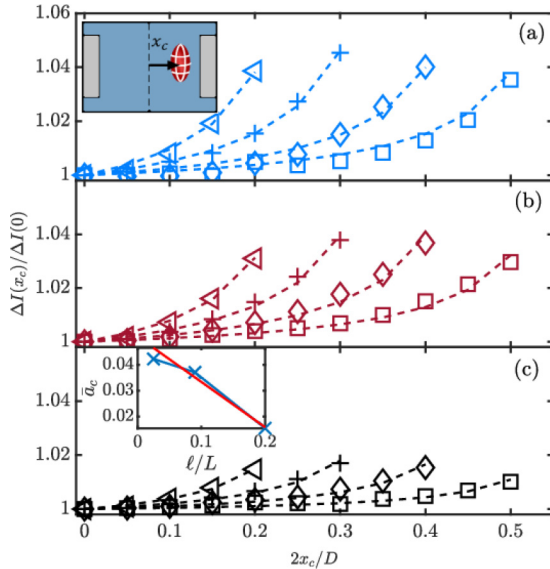


FIG. 8. The ratio of the ionic current difference, $\Delta I(x_c)/\Delta I(0)$, due to the off-axis displacement of the particle vs its position x_c for different spheroid dimensions: (a) $\ell/L = 0.025$, (b) $\ell/L = 0.09$, and (c) $\ell/L = 0.2$. Symbols show the calculated data (\square corresponds to $d/D = 0.4$, \diamond - $d/D = 0.5$, \times - $d/D = 0.6$, \triangleleft - $d/D = 0.7$) while the dashed curves are the results of the data fitting with Eq. (19).

the random thermal fluctuations of the measured ionic current baseline could easily mask this change so that the information about the transverse position of the translocating object may be difficult to extract from the current traces.

To construct a fitting function describing the observed behavior of the ionic current vs x_c , we note that displacing a small particle with the electric potential given by Eq. (A6) by a distance $x_c \ll D/2$ from the nanopore's center decreases the current $I_b^{(2)}$ by $\approx 12A\pi P x_c^2/D^3$ where the particle's induced dipole moment P is given by Eq. (A7). To account for an increase of the electric field next to the particle's side closest to the nanopore, at distances $\sim d + x_c$ from the pore's center, following Smythe [25], we approximate the enhanced electric field in that region by that of the particle with a larger diameter of $d + 2x_c$ located at the center of the pore. Combining these two effects leads to the following fitting formula for the ratio of the differences in the ionic current $\Delta I(x_c)/\Delta I(0)$:

$$\frac{\Delta I(x_c)}{\Delta I(0)} = 1 + a_c \frac{2x_c/D}{1 - (d + 2x_c)/D} \left(\frac{d}{D}\right)^2, \quad (19)$$

where a_c is a fitting parameter. As seen from the inset in Fig. 8(c), this parameter depends only on the nanoparticle's length ℓ . We found that setting $a_c = 0.04 - 0.13\ell/L$ provides the best fits for all calculated data (within 2%, dashed curves in Fig. 8). The above fitting formula obviously breaks down when the nanoparticle touches the surface ($d + 2x_c = D$) but this is likely not a very realistic scenario for an object translocating through a nanopore rather than sticking to its surface.

Note that we did not consider here the effects on the ionic current due to the changes in the angular orientation of the nanoparticle located close to the nanopore surface. This is because, as was already shown, the calculated changes in the ionic current are rather small as it is (within 5%), so that any further orientation-induced contributions to the current blockade are expected to be even smaller.

B. Experimental ramifications

The above discussion focuses on the large-particle corrections to the ionic current. To illustrate the behavior of the ionic current, in the following figure (Fig. 9), we plot the ionic current blockade ratio, $\Delta I/I_o$, for parallel and perpendicular orientations of the translocating spheroidal nanoparticle in the nanopore. Only results for particle lengths $\ell/L \leq 0.09$ are shown as longer particles cannot fully turn in our nanopore. As the diameter increases, the particle's shape changes from the prolate to the oblate, for the green and red symbols and curves with $\ell/L = 0.05$ and 0.025 while all data points for $\ell/L = 0.09$ (blue symbols and curve) correspond to the prolate spheroids, except for the last point with $d/D = 0.9$ for which $d = \ell$ and the particle is a sphere. One can see that for all nonspherical shapes, $\Delta I_{\perp} \neq \Delta I_{\parallel}$, that is, as the particle translocates through the pore, tumbling through it [33], there will be variations in the current due to its random orientation with respect to nanopore axis. Specifically, for the prolate particles, $\Delta I_{\perp} > \Delta I_{\parallel}$ while for the oblate ones, the opposite is true, and the greater the deviations from the spherical shape, the larger the difference between the blocked currents.

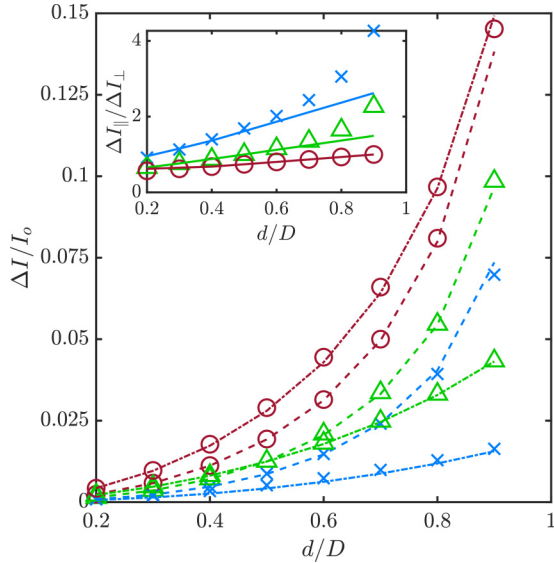


FIG. 9. The ionic current blockade ratios $\Delta I/I_0$ vs the particle diameter d/D for the parallel (\circ) and perpendicular (\times) orientations of the spheroids in the nanopore. Blue dashed lines and symbols correspond to the particle length of $\ell/L = 0.025$, green – $\ell/L = 0.05$, and red – $\ell/L = 0.09$. Inset shows ratio of $\Delta I_{\parallel}/\Delta I_{\perp}$ for the same three lengths with dashed lines showing the small-particle limit of $\Delta I_{\parallel}/\Delta I_{\perp} = f_{\parallel}/f_{\perp}$.

The orientation difference between the ionic currents can be further elucidated by plotting the ratio $\Delta I_{\parallel}/\Delta I_{\perp}$ and comparing it with the small-particle limit where this ratio is equal to f_{\parallel}/f_{\perp} , see Eq. (1). This is shown in the inset to Fig. 9, where one can see that the computed ratio can be as large as ~ 4 for a large and flat, disklike particle. On the other hand, for most of the prolate spheroids, $\Delta I_{\parallel}/\Delta I_{\perp}$ close to the small-particle limit value f_{\parallel}/f_{\perp} , that is, the large-particle corrections play a more significant role for the oblate particles.

One can also use our fitting formulas in conjunction with experimental data on the ionic current blockade values to establish the dimensions of the translocating particles. In general, due to complexity of formulas, this will result in a system of algebraic equations to figure out plausible values of the spheroid's length and diameter. However, some beforehand knowledge of the geometry of the translocating object would be helpful to cut down on the number of possible combinations of d and ℓ , and, for example, in a case of a very long and slender spheroid with $\ell \gg d$ and $\ell \gg D$ this solution can be easily accomplished. To demonstrate this, we first note that in this case the particle can only translocate parallel to the nanopore's axis so that Eq. (15) simplifies to $\Delta I/I_0 = \Omega[1 - 0.71(d/D)^2]$ where we set the shape factor $f_{\parallel} = 1$ [14]. If one performs ionic current blockade measurements for two pores, then using the ratio of $\Delta I_1/\Delta I_2$ the nanoparticle's diameter d can be extracted, and from the either of ΔI values, the length ℓ can be determined. For example, in Ref. [5], for the long rods, it was found that $(\Delta I/I_0)_1 \approx 0.014$ and $(\Delta I/I_0)_2 \approx 0.006$ for pores with diameters 0.77 and 1.2 μm . Using the just outlined procedure, one can then find the rod's diameter to be $d \approx 0.22 \mu\text{m}$ consistent with reported value of 0.21 μm .

V. SUMMARY

In this work we theoretically considered translocation of the spheroidal nanoparticles (oblate and prolate ellipsoids) of various dimensions through a cylindrical nanopore. We focused our attention on neutral particles permeating through an uncharged nanopore which are frequent enough cases observed experimentally, and with help of the numerical solution of the PNP system of equations in 2D and 3D domains, we computed the ionic current through the nanopore with a nanoparticle blocking it. The resulting values of the ionic current blockade were then carefully analyzed vs dimensions of the translocating spheroid, its orientation, and position inside the nanopore.

We found that with increasing size of the nanoparticle, the ionic current reacts differently depending on the orientation of the particle's axis of revolution relative to the nanopore axis. In case of their parallel orientation, the ionic current blockade ratio exhibits a much weaker dependence on the nanoparticle's length than when the two axes are perpendicular to each other. Displacing the nanoparticle off the nanopore's center towards its surface resulted in further reduction of the ionic current (stronger current blockade) dependent on the position of the nanoparticle but remaining within 5% and becoming smaller with increasing length. To make sense of all these results, we also developed a semiempirical model accounting for changes in the electric field inside the nanopore when a large spheroidal particle is present. Using this model, we constructed one parameter fitting formulas for the ionic current blockade values that generally agree with our computed data within 2–4%.

The provided formulas can be extrapolated to other nanoparticle's dimensions not specifically considered in this work to extract, for example, information about nanoparticle's dimensions and shape from the known ionic current traces. This is possible because in case of the neutral particle-pore system, the ionic current blockades depend only on the ratios of nanoparticle and nanopore sizes; this fact was verified by performing 2D and 3D calculations on systems with different dimensions and by applying the proposed formulas to analysis of the experimental data on translocation of rodlike particles. However, when the surface charge on the nanopore-nanoparticle is taken into account, the ionic current response of the nanopore becomes more complicated even for small objects, so that the case of large charged nanoparticles will be considered separately.

APPENDIX A: IONIC CURRENT BLOCKADE FOR LARGE SPHEROIDAL PARTICLES

We next use this approach to find out the correction factors when a large spheroidal particle is blocking the nanopore. To this end, we compute the ionic current from the Ohm's law at $z = 0$ for spheroids of prolate and oblate shapes and with the axis of revolution along and perpendicular to the nanopore axis.

For the case of the prolate ellipsoid ($\ell > d$) with the axis of the revolution parallel to the nanopore axis, the exact solution of Eqs. (10) with zero right-hand side can be written in terms of the prolate spheroidal coordinates defined in Morse and

Feshbach [34] as

$$\phi_0 = -\frac{1}{2}Aa\eta[\xi - BQ_1^0(\xi)], \quad (\text{A1})$$

where $Q_1^0(\xi)$ is the Legendre function of the second kind and a is the interfocal distance, $a = (\ell^2 - d^2)^{1/2}$. Constant B can be evaluated on the surface of the ellipsoid $\xi = \xi_0 =$

$$I_b^{(2)} = 2\pi\sigma \int_{d/2}^{D/2} E_z x dx = -\pi a\sigma \int_{\xi_0}^{\xi_1} \frac{d\phi_0}{d\eta} d\xi = \frac{1}{4}\pi\sigma AD^2 \left[1 - \left(\frac{d}{D}\right)^2 \frac{2\xi_0 - (\xi_0^2 - 1) \ln[(\xi_0 + 1)/(\xi_0 - 1)]}{2\xi_1 - (\xi_1^2 - 1) \ln[(\xi_1 + 1)/(\xi_1 - 1)]} \right], \quad (\text{A2})$$

where $\xi_1 = [(D/a)^2 + 1]^{1/2}$.

From this general expression, following the above procedure, we can then find constant A in limiting cases of interest:

(i) For a very long and slender ellipsoid ($\ell \gg d$ and $\ell \gg D$) that can only translocate through the nanopore with its major axis parallel to the pore axis, both ξ_0 and ξ_1 are ≈ 1 , and we find

$$A \approx \frac{\Delta V}{L} \left[1 - \left(\frac{d}{D}\right)^2 \right]^{-1}. \quad (\text{A3})$$

(ii) On the other hand, for a small and slender ellipsoid when $D \gg \ell \gg d$, that can in principle fully rotate inside the nanopore,

$$A \approx \frac{\Delta V}{L} \left(1 - \frac{2\ell d^2}{3D^3} \right)^{-1}. \quad (\text{A4})$$

By comparing these two expressions, we can see that as the ellipsoid's length increases, the large-particle correction to the ionic current eventually saturates and becomes independent of its length, i.e., the large-particle correction factor changes its leading term dependence from $F[l^2/D^3]$ to $F[(d/D)^2]$.

For the oblate ellipsoid on the pore's axis ($\ell < d$, $\theta = 0$), we can use a similar approach to get the ionic current but in the oblate spheroidal coordinates [34]. This leads to the expression for $I_b^{(2)}$ identical to Eq. (A2) in which $\xi \rightarrow i\xi$, $\xi_0^2 = (d/2a)^2 - 1$, $\xi_1^2 = (D/2a)^2 - 1$, and $a = (d^2 - l^2)^{1/2}/2$.

As a limiting case, we consider here only the case of a small, disklike, ellipsoid with $\ell \rightarrow 0$ and $d \approx 2a \ll D$, for which we find that

$$A \approx \frac{\Delta V}{L} \left(1 - \frac{4d^3}{3\pi D^3} \right)^{-1}, \quad (\text{A5})$$

that is, the ionic current correction is given by $F[(d/D)^3]$, as is for the spherical particles of the same diameter, see Eq. (7).

To perform calculations for the perpendicular orientation of small spheroids to the nanopore axis, angle $\theta = 90^\circ$ [35], we note that for small nanoparticles, the main contribution to the ionic current in Eq. (A2) comes from the electric field (current density) away from the particle, at distances large enough compared to its dimensions. For prolate spheroids, in this case, coordinates $\xi \approx 2r/a$ and $\eta \approx z/r = \cos\theta$ where r is the distance from the center of the spheroid. Since $Q_1^0(\xi \gg 1) \approx (3\xi^2)^{-1}$, at large distances from the particle, potential ϕ_0 given by Eq. (A1) becomes approximately equal to that one of

$[(d/a)^2 + 1]^{1/2}$ from the boundary condition (13) $\partial\phi_0/\partial n = (1/h_\xi)(\partial\phi_0/\partial\xi)|_{\xi_0} = 0$ as $B = [\frac{d}{d\xi}Q_1^0(\xi)|_{\xi_0}]^{-1}$.

To evaluate the blocked pore current at $z=y=a\xi\eta/2=0$, we set $\eta = 0$ so that $x = a(\xi^2 - 1)^{1/2}/2$ and $E_z = -(2/a\xi)(\partial\phi_0/\partial\eta)$. The ionic current from the Ohm's law [Eq. (6)] is then

the electric dipole P in the uniform electric field:

$$\phi_0 \approx -A \cos\theta \left(r - \frac{P}{r^2} \right). \quad (\text{A6})$$

The dipole moment P of the spheroid can be found from the general expression in Ref. [36] for the classical problem of the dielectric ellipsoid in the uniform electric field [setting $\epsilon^{(i)} = 0$ in that expression to satisfy boundary condition (13)] as:

$$P = -\frac{ld^2}{24(1-n)}, \quad (\text{A7})$$

where n is the depolarization (demagnetization) factor along a specific direction—in this case, parallel to the nanopore axis, $n = n_{\parallel}$. For a small slender prolate spheroids [37], $n_{\parallel} \approx (d/l) \ln(2l/d) \ll 1$, so that substitution of the above electric potential in Eq. (6) immediately produces the same result for constant A as given by Eq. (A4). Performing the same calculation for the oblate spheroids (in the oblate spheroidal coordinates, large $\xi \approx r/a \gg 1$ and $n_{\parallel} \approx 1 - \pi l/(2d)$ [37]) reproduces the result of Eq. (A5).

For the perpendicular orientation of spheroids in the nanopore, we then use the depolarization factor $n = n_{\perp}$ along a direction perpendicular to the nanopore's axis:

(i) For a slender prolate spheroid, $n_{\perp} \approx 1/2$ [37], and we find that

$$A \approx \frac{\Delta V}{L} \left(1 - \frac{4ld^2}{3D^3} \right)^{-1}. \quad (\text{A8})$$

(ii) For a flat oblate spheroid, $n_{\perp} \approx \pi l/(4d) \ll 1$ [37], and

$$A \approx \frac{\Delta V}{L} \left(1 - \frac{2ld^2}{3D^3} \right)^{-1}. \quad (\text{A9})$$

APPENDIX B: VALIDATION OF THE MODEL

We first compare our computed ionic currents for the spherical nanoparticles of different diameters from 2D and 3D models. To emphasize the importance of the large-particle correction term, in Fig. 10 we plot a ratio of $\Delta I/I_0$ and $f\Omega$ vs particle diameter extracted from 2D and 3D simulations. An excellent agreement between the two data sets (within 2%) for $d/D > 0.1$ is found suggesting that our procedure for scaling down the system for 3D calculations works well in this range of particle sizes. This is as expected because the equations for $\Delta I/I$ and large-particle corrections derived in Appendix A depend only on the ratios of the particle and pore

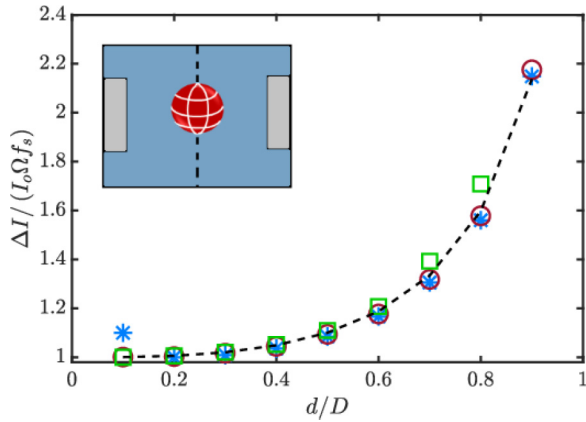


FIG. 10. The large-particle correction term $\Delta I/(I_o\Omega f_s)$ for spherical nanoparticles. Blue and red symbols are the results of 3D and 2D calculations, green symbols are results of Ref. [38], and the dashed curve is the semiempirical data fit by Eq. (B1).

dimensions. It is also seen in this plot that for the smallest studied nanoparticle with $d/D = 0.1$, 2D and 3D calculations deviate, with 2D calculations clearly producing more accurate results, likely because our mesh in 3D case is too coarse to get accurate data for the current change due such a small object. Because of this, all subsequent calculations in this work are limited to $d/D \geq 0.2$.

In the same figure, we also compare our numerically computed results with analytic calculations of Smythe [38] for the flow around a spheroid in a cylindrical tube (green symbols in Fig. 10). A good agreement for smaller particles is found but deviations between our numerical results and those of Ref. [38] appear with increase of the particle's size with our data being smaller by about 9% for the largest considered nanoparticle size.

Based on the results for spherical particles [Eq. (8)], one can propose a one-parameter fitting formula for the ionic current blockade covering all nanoparticle sizes as

$$\frac{\Delta I}{I_o f \Omega} = \left[1 - a_s \left(\frac{d}{D} \right)^3 \right]^{-1} \quad (\text{B1})$$

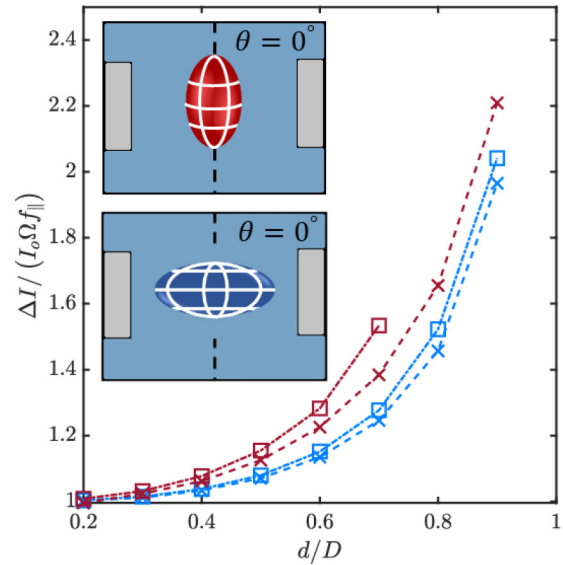


FIG. 11. Normalized ionic current blockade ratio $\Delta I/(I_o\Omega f_{||})$ for prolate (red) and oblate (blue) ellipsoids with $\ell:d$ ratios 2:1 and 1:2. Squares (connected with dotted lines) represent the results of our calculations while crosses (with dashed lines) are the results of the calculations of Ref. [40].

with a_s being a fitting parameter. The same relation between $\Delta I/I_o$ and d/D was also proposed in earlier works [20,39]. We found that the value of $a_s = 0.73$ fits our data best (within 3%, the black dashed curve in Fig. 10), in excellent agreement with usually accepted value of this parameter [20,39].

We also compared our numerically computed $\Delta I/I_o$ values with calculations of Smythe [40] for prolate and oblate ellipsoids with ratios $\ell : d = 2 : 1$ and $1 : 2$ with axes of revolution oriented along the nanopore axis. The results for $\Delta I/(I_o\Omega f_{||})$ are shown in Fig. 11 where one can see that the agreement between our calculations and those of Ref. [40] is quite good for the oblate ellipsoid (within 2%) for the whole range of the particle diameters d . However, for the prolate spheroids, the agreement is worse particularly at larger particle sizes. This is likely due to the decreasing accuracy in calculations for the prolate spheroids noted in Ref. [40].

- [1] W. H. Coulter, Means for counting particles suspended in a fluid, United States Patent: 2656508 (1953).
- [2] R. W. DeBlois and C. P. Bean, Counting and sizing of sub-micron particles by the resistive pulse technique, *Rev. Sci. Instrum.* **41**, 909 (1970).
- [3] W. Hogg and W. H. Coulter, Apparatus and method for measuring a dividing particle size of a particulate system, United States Patent: 3557352 (1971).
- [4] R. dela Torre, J. Larkin, A. Singer, and A. Meller, Fabrication and characterization of solid-state nanopore arrays for high throughput DNA sequencing, *Nanotechnology* **23**, 385308 (2012).
- [5] Y. Qiu, P. Hinkle, C. Yang, H. E. Bakker, M. Schiel, H. Wang, D. Melnikov, M. Gracheva, M. E. Toimil-Molares, A. Imhof,

and Z. S. Siwy, Pores with longitudinal irregularities distinguish objects by shape, *ACS Nano* **9**, 4390 (2015).

- [6] W. Si and A. Aksimentiev, Nanopore sensing of protein folding, *ACS Nano* **11**, 7091 (2017).
- [7] A. J. McMullen, J. X. Tang, and D. Stein, Nanopore measurements of filamentous viruses reveal a sub-nanometer-scale stagnant fluid layer, *ACS Nano* **11**, 11669 (2017).
- [8] S. Sensale, C. Wang, and H.-C. Chang, Resistive amplitude fingerprints during translocation of linear molecules through charged solid-state nanopores, *J. Chem. Phys.* **153**, 035102 (2020).
- [9] G. Xi, Y. Ye, L. Wang, W. Zhuang, X. Yan, Y. Wang, L. Zhang, and L. Wu, Spatial conformation measurement of gold nanorods

- translocated through a solid-state nanopore, *Mater. Express* **10**, 1732 (2020).
- [10] M. Drndić, 20 years of solid-state nanopores, *Nat. Rev. Phys.* **3**, 606 (2021).
- [11] C. L. Rice and R. Whitehead, Electrokinetic flow in a narrow cylindrical capillary, *J. Phys. Chem.* **69**, 4017 (1965).
- [12] J. Sha, W. Si, B. Xu, S. Zhang, K. Li, K. Lin, H. Shi, and Y. Chen, Identification of spherical and nonspherical proteins by a solid-state nanopore, *Anal. Chem.* **90**, 13826 (2018).
- [13] C. Ying, J. Houghtaling, and M. Mayer, Effects of off-axis translocation through nanopores on the determination of shape and volume estimates for individual particles, *Nanotechnology* **33**, 275501 (2022).
- [14] D. C. Golibersuch, Observation of aspherical particle rotation in Poiseuille flow via the resistance pulse technique. II. application to fused sphere “dumbbells,” *J. Appl. Phys.* **44**, 2580 (1973).
- [15] L. I. Berge, J. Feder, and T. Jossang, A novel method to study single-particle dynamics by the resistive pulse technique, *Rev. Sci. Instrum.* **60**, 2756 (1989).
- [16] L. I. Berge, Particle transit time distributions in single pores by the resistive pulse technique, *J. Colloid Interface Sci.* **135**, 283 (1990).
- [17] R. Maugi, P. Hauer, J. Bowen, E. Ashman, E. Hunsicker, and M. Platt, A methodology for characterising nanoparticle size and shape using nanopores, *Nanoscale* **12**, 262 (2020).
- [18] G. R. Willmott, Tunable resistive pulse sensing: Better size and charge measurements for submicrometer colloids, *Anal. Chem.* **90**, 2987 (2018).
- [19] R. Pan, K. Hu, R. Jia, S. A. Rotenberg, D. Jiang, and M. V. Mirkin, Resistive-pulse sensing inside single living cells, *J. Am. Chem. Soc.* **142**, 5778 (2020).
- [20] R. W. DeBlois, C. P. Bean, and R. K. Wesley, Electrokinetic measurements with submicron particles and pores by the resistive pulse technique, *J. Colloid Interface Sci.* **61**, 323 (1977).
- [21] J. E. Hall, Access resistance of a small circular pore, *J. Gen. Physiol.* **66**, 531 (1975).
- [22] J. Wang, J. Ma, Z. Ni, L. Zhang, and G. Hu, Effects of access resistance on the resistive-pulse caused by translocating of a nanoparticle through a nanopore, *RSC Adv.* **4**, 7601 (2014).
- [23] N. Grover, J. Naaman, S. Ben-Sasson, and F. Doljanski, Electrical sizing of particles in suspensions: I. Theory, *Biophys. J.* **9**, 1398 (1969).
- [24] J. Hurley, Sizing particles with a Coulter counter, *Biophys. J.* **10**, 74 (1970).
- [25] W. R. Smythe, Off-axis particles in Coulter type counters, *Rev. Sci. Instrum.* **43**, 817 (1972).
- [26] L. I. Berge, T. Jossang, and J. Feder, Off-axis response for particles passing through long apertures in Coulter-type counters, *Meas. Sci. Technol.* **1**, 471 (1990).
- [27] Z. Qin, J. Zhe, and G.-X. Wang, Effects of particle’s off-axis position, shape, orientation and entry position on resistance changes of micro Coulter counting devices, *Meas. Sci. Technol.* **22**, 045804 (2011).
- [28] Z. K. Hulings, D. V. Melnikov, and M. E. Gracheva, Brownian dynamics simulations of the ionic current traces for a neutral nanoparticle translocating through a nanopore, *Nanotechnology* **29**, 445204 (2018).
- [29] D. V. Melnikov, Z. K. Hulings, and M. E. Gracheva, Concentration polarization, surface charge, and ionic current blockade in nanopores, *J. Phys. Chem. C* **124**, 19802 (2020).
- [30] K. E. Venta, M. B. Zanjani, X. Ye, G. Danda, C. B. Murray, J. R. Lukes, and M. Drndić, Gold nanorod translocations and charge measurement through solid-state nanopores, *Nano Lett.* **14**, 5358 (2014).
- [31] S. Qian and Y. Ai, *Electrokinetic Particle Transport in Micro-/Nanofluidics Direct Numerical Simulation Analysis* (CRC Press, Boca Raton, FL, 2012).
- [32] H. Zhao and H. H. Bau, The polarization of a nanoparticle surrounded by a thick electric double layer, *J. Colloid Interface Sci.* **333**, 663 (2009).
- [33] C. Wells, D. V. Melnikov, and M. E. Gracheva, Brownian dynamics of cylindrical capsule-like particles in a nanopore in an electrically biased solid-state membrane, *Phys. Chem. Chem. Phys.* **24**, 2958 (2022).
- [34] P. M. Morse and H. Feshbach, *Methods of Theoretical Physics* (McGraw–Hill, New York, 1953).
- [35] The direct evaluation of the ionic current in this case leads to a rather cumbersome calculations due to the lack of the circular symmetry in the cross-sectional area of the pore open to the current flow at the position of the ellipsoid.
- [36] L. D. Landau and E. M. Lifshitz, *Electrodynamics of Continuous Media* (Pergamon, New York, 1984).
- [37] J. A. Osborn, Demagnetizing factors of the general ellipsoid, *Phys. Rev.* **67**, 351 (1945).
- [38] W. R. Smythe, Flow around a sphere in a circular tube, *Phys. Fluids* **4**, 756 (1961).
- [39] J. L. Anderson and J. A. Quinn, The relationship between particle size and signal in Coulter-type counters, *Rev. Sci. Instrum.* **42**, 1257 (1971).
- [40] W. R. Smythe, Flow around a spheroid in a circular tube, *Phys. Fluids* **7**, 633 (1964).